THE JOURNAL OF PHYSICAL CHEMISTRY Letters

Letter

pubs.acs.org/JPCL

Full-Dimensional Quantum State-to-State Nonadiabatic Dynamics for Photodissociation of Ammonia in its *A*-Band

Changjian Xie,[†] Jianyi Ma,*[,‡,§] Xiaolei Zhu,[∥] Dong Hui Zhang,[⊥] David R. Yarkony,*[,∥] Daiqian Xie,*[,†,#] and Hua Guo*[,‡]

[†]Institute of Theoretical and Computational Chemistry, Key Laboratory of Mesoscopic Chemistry, School of Chemistry and Chemical Engineering, Nanjing University, Nanjing 210093, China

[‡]Department of Chemistry and Chemical Biology, University of New Mexico, Clark Hall 101, Albuquerque, New Mexico 87131, United States

[§]Institute of Atomic and Molecular Physics, Sichuan University, Chengdu, Sichuan 610065, China

[∥]Department of Chemistry, Johns Hopkins University, 3400 North Charles Street, Baltimore, Maryland 21218, United States

[⊥]State Key Laboratory of Molecular Reaction Dynamics and Center for Theoretical and Computational Chemistry, Dalian Institute of Chemical Physics, Chinese Academy of Science, 457 Zhongshan Road, Dalian 116023, China

[#]Synergetic Innovation Center of Quantum Information and Quantum Physics, University of Science and Technology of China, Hefei, Anhui 230026, China

Supporting Information

ABSTRACT: Full-dimensional state-to-state quantum dynamics of the photodissociation of $NH_3(\tilde{A}^1A_2'')$ is investigated on newly developed coupled diabatic potential energy surfaces. For the first time, the rovibrational distributions of the nonadiabatically produced $NH_2(\tilde{X}^2B_1)$ product have been determined quantum mechanically. In agreement with experimental observations, $NH_2(\tilde{X}^2B_1)$ produced from the 0^0 and 2^1 states of $NH_3(\tilde{A}^1A_2'')$ was found to be dominated by its ground vibrational state with an $N = K_a$ propensity, shedding light on the quantum-state-resolved nonadiabatic dynamics facilitated by conical intersections and setting the stage for the elucidation of vibrationally mediated photodissociation.

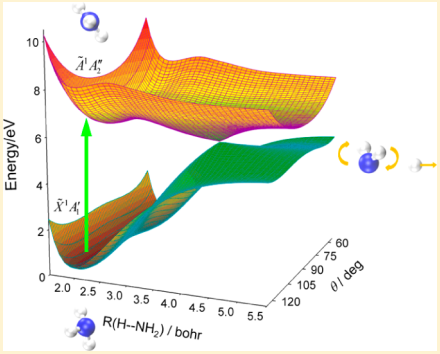

SECTION: Spectroscopy, Photochemistry, and Excited States

The breakdown of the Born−Oppenheimer approximation in molecular systems is responsible for many important chemical processes, including vision and photosynthesis. Conical intersections (CIs) are the primary cause for the failure of the Born−Oppenheimer approximation.[1−3] Advances in our understanding of nonadiabatic dynamics have relied heavily on prototypical systems where the electron−nuclear interactions can be accurately characterized. Photodissociation of small molecules provides such an ideal proving ground.[4,5] Indeed, we have recently demonstrated that state-to-state multichannel quantum nonadiabatic dynamics of the photodissociation of water in its second absorption band can be quantitatively understood by wave-packet dynamics on accurate coupled potential energy surfaces (PESs).[6−8]

The photodissociation of ammonia in its *A*-band, which has been the object of innumerable experimental and theoretical studies over the past 30 years, provides another archetypical example of nonadiabatic dynamics.[4] Its six internal degrees of freedom offer dynamical features richer than those in the triatomic water molecule. In addition to the adiabatic dissociation channel leading to the H + $NH_2(\tilde{A}^2A_1)$ products, nonadiabatic dissociation of photoexcited $NH_3(\tilde{A}^1A_2'')$ through a seam of CIs between the ground and first excited electronic states of NH_3 leads to the lower energy H + $NH_2(\tilde{X}^2B_1)$ products. As a result, it serves as an attractive system to understand, at the state-to-state level, multidimensional nonadiabatic dynamics and an array of other important dynamical properties including tunneling, mode specificity, and intramolecular vibrational energy redistribution (IVR).

It is well established that the $\tilde{A}\leftarrow\tilde{X}$ absorption spectrum of ammonia is dominated by a long progression corresponding to umbrella mode (2^n) excitations, which are attributed to the pyramidal-to-planar transition.[9] The diffuse characteristic of the absorption peaks reflects strong predissociation on the excited electronic state due to a small barrier just outside the quasi-bound Franck−Condon (FC) region. Lifetimes of these

Received: February 1, 2014
Accepted: March 10, 2014
Published: March 10, 2014

tunneling facilitated resonances were found to range from femtoseconds to picoseconds, depending on the rovibrational quantum number and isotopic substitutions. The nonadiabatic transitions are the consequence of a CI seam between the $\tilde{X}$ and $\tilde{A}$ states of NH_3, a point on which is shown in Figure 1.

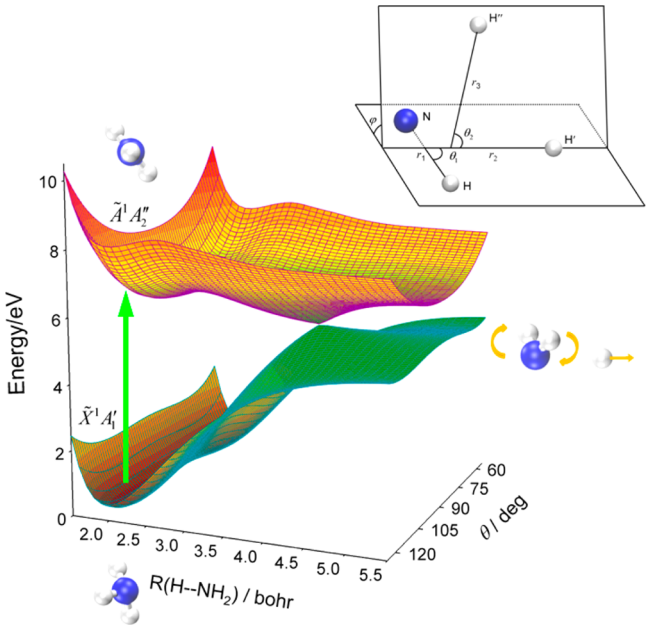

Figure 1. Adiabatic potential energy surfaces of ammonia as a function of R(N−H) and the out-of-plane angle θ. The Jacobi coordinates used in the calculations are also depicted.

In addition to absorption spectra,[9−13] product-state distributions of $NH_2(\tilde{A}^2A_1/\tilde{X}^2B_1)$ have been determined experimentally by several groups.[14−26] The fact that $NH_2(\tilde{X}^2B_1)$ produced by the nonadiabatic channel dominates at most photon frequencies underscores the central role of the CIs in the dissociation dynamics. Other observations important in the present context include the $(0, \nu_2 = 0-1, 0)$ and $N \approx K_a$ propensities for the $NH_2(\tilde{X}^2B_1)$ fragment and drastically different $NH_2(\tilde{X}^2B_1)$ rotational state distributions between dissociations from the 0^0 and 2^1 states of NH_3.[14−16,18,23,26] (N and K_a are the rotational quantum number (excluding spin) and its projection onto the a axis of NH_2.) These rovibrationally resolved measurements have yet to be elucidated theoretically. This deficiency acquires increased significance because rotational energy distributions also play an essential role in analyzing the vibrationally mediated photodissociation of NH_3, which to date has resisted attempts at explanation.[21−23]

The abundant experimental data on this system pose a challenge to theory. Indeed, there has been a plethora of theoretical studies of the ammonia photodissociation dynamics over the last three decades.[27−34] These reduced-dimensionality models have not only shed valuable light on this prototypical system but also helped to establish a better understanding of nonadiabatic dynamics in general. However, a definitive characterization of the rovibrationally resolved state-to-state nonadiabatic dynamics of ammonia photodissociation requires a full-dimensional quantum mechanical treatment based on accurate PESs. It is only recently that a truly ab initio treatment with full dimensionality has become possible, thanks to advances in electronic structure calculations, coupled PES fitting,[35−38] and quantum dynamics.[39,40] Indeed, some of the current authors have recently reported a first-principles full-dimensional treatment of ammonia photodissociation that yielded excellent agreement with the measured absorption spectra of both the NH_3 and ND_3 isotopomers[38] and with the estimated branching ratios between the two dissociation channels, $NH_2(\tilde{X}^2B_1)$ and $NH_2(\tilde{A}^2A_1)$.[41] However, experimental values of branching ratios were estimated from the kinetic energy distribution of the products, resulting in a large margin of error. To facilitate a direct comparison with experiment, the kinetic energy distribution of the products needs to be simulated, which requires rovibrational resolution of the NH_2 product.

Although the resolution of the rovibrational levels of the $NH_2(\tilde{X}^2B_1)$ fragment, which can provide a sensitive assessment of the accuracy of the nonadiabatic dynamics involving the CI seam, is extremely challenging due to the large grid needed and to the numerous internal states made accessible by the large excess energy, recent advances in quantum-state-resolved full-dimensional dynamics of tetra-atomic systems[42,43] have made possible the current treatment. We report the first full-dimensional quantum mechanical determination of the $NH_2(\tilde{X}^2B_1)$ internal state distribution upon the photodissociation of NH_3. This is achieved by introducing an improved set of diabatic PESs and a different scattering coordinate system from that used in our previous work.[34,38,39,41]

A previously constructed 2 × 2 quasi-diabatic representation of the 1^1A and 2^1A state PESs of ammonia[41] is reconstructed with an improved fitting algorithm and augmented data set. A null-space analysis procedure is adopted to redesign the coordinate expansion, and a partially diagonalized representation is introduced to facilitate better description of near-degeneracy data points. These methods are described in detail in a recent publication,[44] where this approach enabled the fitting of the phenol $1,2,3^1A$ coupled PESs including all 33 degrees of freedom.

The previous diabatic PESs contained 9652 symmetrized basis matrices (linear parameters). The null-space analysis revealed a large nullity of ∼5000. The previous PESs also experience oscillations at very short bond lengths, created by high-order terms of exponential functions. The new expansion, redesigned with the help of the null-space analysis procedure, contains only 2762 basis matrices with a small nullity of 240. The new PESs are free of artificial oscillations at short bond distances. The single-coordinate functions used in the new fit are described in Supporting Information (SI). Despite the significantly smaller expansion size, the fitting errors in energies, energy gradients, and derivative couplings are smaller for points with energies above 40 000 cm^{-1} and are nearly unchanged for other geometries with lower energies. One million test quasi-classical surface hopping trajectories were generated from a large number of different initial conditions. No trajectory was found to leave the region defined by existing data points or discover any holes on the PESs.

The PES needs to be extremely flat and accurate in the asymptote to obtain correct rovibrational states of the NH_2 product. Ab initio data from 332 new geometries were added to the data set, the majority of which are near the NH_2 + H or NH + H_2 asymptotes. The scaling parameter of the out-of-plane coordinate was also adjusted to ensure flatness in the asymptotes.

To make the assignments easier for the rovibrational states of the $NH_2(\tilde{X}^2B_1)$ product, we chose the Jacobi coordinates

dx.doi.org/10.1021/jz500227d | J. Phys. Chem. Lett. 2014, 5, 1055−1060

Table 1. Calculated Energy Levels (cm^{-1}) of $NH_2(\tilde{X}^2B_1)$ Rovibrational States with $(0, \nu_2, 0)$, $N = K_a$

	ν_2					
	0			1		
K_a	calc.[a]	obs.[b]	calc. (this work)	calc.[a]	obs.[b]	calc. (this work)
0	0	0	0.00	1495	1497.32	1492.15
1	34	34.28	31.96	1532	1533.85	1526.25
2	116	116.29	117.77	1620	1622.50	1618.82
3	244	244.36	245.57	1758	1761.22	1757.29
4	417	417.91	419.93	1944	1948.75	1945.61
5	634	635.61	638.43	2177	2183.20	2180.76
6	893	895.95	899.72	2455	2462.10	2460.65
7	1194	1197.20	1202.10	2774	2783.61	2782.95
8	1533	1537.60	1543.83	3133	3144.94	3145.35
9	1910	1915.39	1923.14	3530	3544.00	3545.63
10	2322	2328.79	2338.29	3962	3978.64	3981.67
11	2768	2776.08	2787.57	4427	4446.91	4451.48
12	3245	3255.55	3269.33	4924	4946.77	4953.21
13	3753	3765.71	3782.01	5450	5476.67	5485.13
14	4290	4304.95	4324.11	6004	6034.82	6045.64
15	4854	4871.93	4894.22	6584	6619.83	6633.23
16	5443	5465.21	5490.99	7189	7230.17	7246.53
17	6057	6083.60	6113.16	7817	7864.65	7884.23
18	6694	6725.80	6759.52	8468	8521.96	8545.12
19	7353	7390.78	7428.95	9139	9201.06	9228.07
20	8032	8077.38	8120.36	9830		9932.01
21	8732	8784.60	8832.74	10539	10618.41	
22	9449		9565.12			
23	10184					

[a]Ref 15. [b]Ref 48.

shown in Figure 1. The nuclear Hamiltonian defined in the diabatic representation is given in the matrix form:[41]

$$\mathbf{H} = \hat{T}\mathbf{I} + \mathbf{V}^d \quad (1)$$

where $\mathbf{I}$ is a 2-D identity matrix and $\mathbf{V}^d$ is the 2 × 2 diabatic potential energy matrix. The kinetic energy operator ($J = 0$) can be written as ($\hbar = 1$)

$$\hat{T} = -\sum_{i=1}^{3} \frac{1}{2\mu_i}\frac{\partial^2}{\partial r_i^2} + \frac{\hat{j}_1^2}{2\mu_1 r_1^2} + \frac{(\hat{j}_2 - \hat{j}_1)^2}{2\mu_2 r_2^2} + \frac{\hat{j}_2^2}{2\mu_3 r_3^2} \quad (2)$$

in which r_1 is the bond length of diatom NH, r_2 is the distance from the center of mass of diatom NH to atom H′, and r_3 is the distance from the center of mass of triatom NHH′ to atom H″. μ_1, μ_2, and μ_3 are the corresponding reduced masses. $\hat{j}_1$ and $\hat{j}_2$ are the angular momentum operators for diatom NH and triatom NHH′, respectively, and the total angular momentum is set to zero. The spin angular momentum is ignored.

The discretization and Chebyshev propagation schemes are similar to our previous work,[41] and thus no details are given. The parameters for the dynamical calculations can be found in the SI. The initial wave packets were taken as the two lowest parity-adapted vibrational state wave functions of NH_3 on its ground electronic state, which have a splitting of 0.66 cm^{-1} due to tunneling. The photodissociation amplitude of a specified rovibrational state for the product NH_2 was obtained from the discrete Fourier transform of the Chebyshev correlation function,[45,46] which was computed in the dissociation asymptote (r_3^{∞} = 10.0 bohr). The 5-D rovibrational states of $NH_2(\tilde{X}^2B_1)$ were obtained from the iterative Lanczos method.[47] The assignments were achieved by inspecting the wave functions and comparing the energy levels with previous theoretical or experimental values. Table 1 lists the calculated rovibrational energy levels of $NH_2(\tilde{X}^2B_1)$ with $(0, \nu_2, 0)$ and $N = K_a$, together with available calculated[15] and observed[48] data. It can be readily seen that the agreement is quite good, thus validating the high accuracy of the PES.

Figure 2a,b displays the internal state distributions of the $NH_2(\tilde{X}^2B_1)$ product at the 0^0 and 2^1 peaks in the absorption spectrum. The $NH_2(\tilde{A}^2A_1)$ + H channel is not open at these wavelengths. Because there are too many (~3300 for 0^0 and ~3770 for 2^1) rovibrational states, only those with large intensities are assigned. It is clear that the theoretical distributions are dominated by rotational excited states of the vibrationless NH_2 with the propensity of $N \approx K_a$; also some $\nu_2 = 1$ states are present. In addition, the NH_2 rotational distribution for the photodissociation from the 2^1 level of NH_3 is inverted when compared with the 0^0 level, with little population in the low rotational states. These results are in good agreement with observations by many experimental groups, as we now explain.[14−16,18,23,26]

In Figure 3a,b, the calculated translational energy distributions for the products are compared with experimental results[14,18,23,26] at the two wavelengths. The calculated distributions were generated by Gaussian convolution with a fixed full width at half-maximum (fwhm) of 200 cm^{-1}.[14] To account for errors in theoretical vertical excitation energy and NH_2−H dissociation energy, we shifted the calculated distributions lower by 320 cm^{-1} to match the experiment distributions. It can be readily seen that both the theoretical and experimental distributions have the rich structures, corresponding to the product rovibrational states. The

dx.doi.org/10.1021/jz500227d | J. Phys. Chem. Lett. 2014, 5, 1055−1060

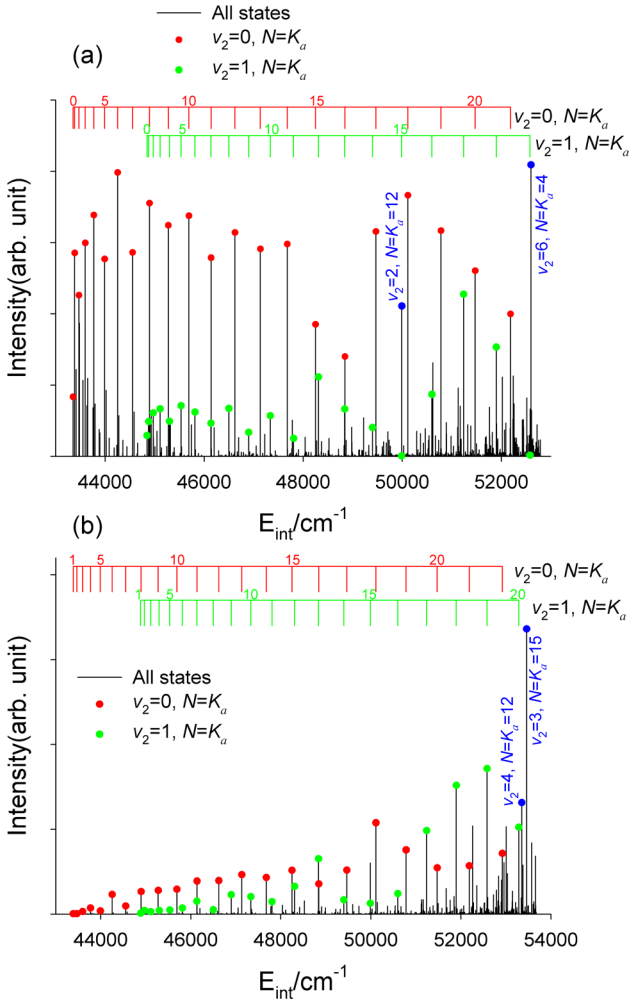

Figure 2. Distributions of the rovibrational states of the $NH_2(\tilde{X}^2B_1)$ product as a function of the internal energy at the total energy of 6.55 eV (a) and 6.66 eV (b), which correspond to the 0^0 and 2^1 states of $NH_3(\tilde{A}^1A_2'')$. The $N = K_a$ rotational states are labeled as red and green dots for $\nu_2 = 0$ and 1, respectively.

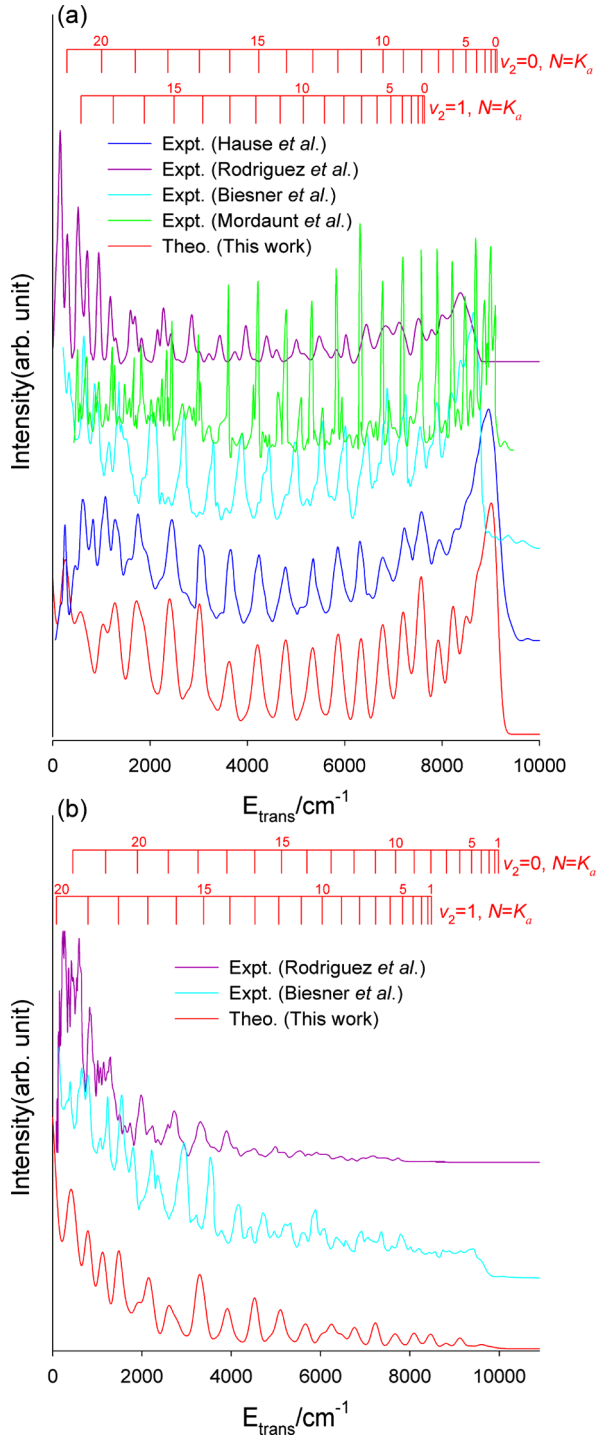

Figure 3. (a) Comparison of the calculated H-translational energy distribution of the $NH_2(\tilde{X}^2B_1)$ product with experimental results of Mordaunt et al. (fwhm = 25 + 0.0007E_{trans} cm^{-1}),[18] Biesner et al.,[14] Hause et al.,[23] and Rodríguez et al.,[26] at the total energy of 6.55 eV (the 0^0 state). (b) Comparison of the calculated H-translational energy distribution of the $NH_2(\tilde{X}^2B_1)$ product with the experimental results of Biesner et al.[14] and Rodríguez et al.[26] at the total energy of 6.66 eV (the 2^1 state). The calculated $N = K_a$ energy levels of $NH_2(\tilde{X}^2B_1)$ are also included. Individual results are shifted for clarity with the theoretical results below those of experiments.

theoretical distributions reproduce the overall shapes and line spacing of the experimental distributions, despite some small differences among the latter. In particular, the translational energy distribution for the 0^0 resonance indicates both slow and fast H atoms, while that for the 2^1 resonance is dominated by slow H atoms due to the inverted NH_2 rotational state distribution previously discussed.

The preeminence of the $N = K_a$ propensity for the $NH_2(\tilde{X}^2B_1)$ product has been discussed previously.[14,15] It can be understood in terms of a simple impulsive model in which the rotational excitation of NH_2 along its *a* axis is attributed to the torque exerted by the recoiling H.[14,30] The slight difference in the HNH bond angles (120 vs 103°) in $NH_3(\tilde{A}^1A_2'')$ and $NH_2(\tilde{X}^2B_1)$ results in some excitation in the NH_2 bending mode. However, because the N−H bond lengths in $NH_3(\tilde{A}^1A_2'')$ are not much different from those in the $NH_2(\tilde{X}^2B_1)$ product, it is not surprising that the product possesses little vibrational excitation in the stretching modes.

The CIs play a profound role in the large differences between the product state distributions for the 0^0 and 2^1 resonances.[14] Because the CIs have C_s symmetry with energy minimization favoring C_{2v} structures,[18,49] the recoil of the H fragment in planar geometries directly through the CIs results in relatively low rotational excitation in NH_2 because the energy release is mostly to the (NH_2−H) translational and vibrational

dx.doi.org/10.1021/jz500227d | *J. Phys. Chem. Lett.* 2014, 5, 1055−1060

coordinates. Fragmentation at nonplanar geometries tends to exert a torque on the departing NH_2 fragment, as nonadiabatic transitions to the ground-state PES take place via avoided crossings.[14,30] Because the wave function of the 0^0 resonance of $NH_3(\tilde{A}^1A_2'')$ has its maximum at a planar geometry, the dissociation is dominated by planar trajectories, thus resulting in a relatively cold NH_2 rotational distribution. The 2^1 state wave function has a node at planarity, leading to the well-known abnormality of the predissociation rate.[9−13] Its dissociation is thus dominated by nonplanar trajectories, which result in the much higher rotational excitation in the NH_2 product.

To summarize, we reported in this work rovibrational state distributions of the $NH_2(\tilde{X}^2B_1)$ product for the photodissociation of ammonia obtained using a full-dimensional non-Born−Oppenheimer quantum wave-packet method on newly developed coupled PESs. The energy levels and product distributions are both in good agreement with the experimental data, thus providing valuable insights into the mechanism and dynamics of the nonadiabatic photodissociation of ammonia at the quantum-state resolved level. This work sets the stage for the elucidation of vibrationally mediated photodissociation of ammonia, in which the product translational distribution suggested a drastic change in the $NH_2(\tilde{A}^2A_1)/NH_2(\tilde{X}^2B_1)$ branching ratio when the ν_3 mode is excited before photolysis.[22]

■ ASSOCIATED CONTENT

Supporting Information

Functional forms and parameters used in the fitting of the PESs and dynamical calculations. This material is available free of charge via the Internet at http://pubs.acs.org.

■ AUTHOR INFORMATION

Corresponding Authors

*J.M.: E-mail: jianyi.m@gmail.com.
*D.R.Y.: E-mail: yarkony@jhu.edu.
*D.X.: E-mail: dqxie@nju.edu.cn.
*H.G.: E-mail: hguo@unm.edu.

Notes

The authors declare no competing financial interest.

■ ACKNOWLEDGMENTS

The NJU and DICP teams were supported by National Natural Science Foundation of China (21133006, 21273104, and 910221301 to D.X. and 21303110 D.H.Z.) and the Ministry of Science and Technology (2013CB834601 to D.X. and D.H.Z.). J.M. acknowledges National Nature Science Foundation of China (21303110). Both the UNM and JHU teams are supported by US DOE (DE-FG02-05ER15694 to H.G. and DE-FG02-91ER14189 to D.R.Y.).

■ REFERENCES

(1) Köppel, H.; Domcke, W.; Cederbaum, L. S. Multimode Molecular Dynamics beyond the Born-Oppenheimer Approximation. *Adv. Chem. Phys.* **1984**, *57*, 59−246.

(2) Bernardi, F.; Olivucci, M.; Robb, M. A. The Role of Conical Intersection and Excited State Reaction Paths in Photochemical Pericyclic Reactions. *J. Photochem. Photobiol. A* **1997**, *105*, 365−371.

(3) Yarkony, D. R. Determination of Potential Energy Surface Intersections and Derivative Couplings in the Adiabatic Representation. In *Conical Intersections: Electronic Structure, Dynamics and Spectroscopy*; Domcke, W., Yarkony, D. R., Köppel, H., Eds.; World Scientific Publishing: Singapore, 2004.

(4) Ashfold, M. N. R.; King, G. A.; Murdock, D.; Nix, M. G. D.; Oliver, T. A. A.; Sage, A. G. $\pi\sigma^*$ Excited States in Molecular Photochemistry. *Phys. Chem. Chem. Phys.* **2010**, *12*, 1218−1238.

(5) Yuan, K.; Dixon, R. N.; Yang, X. Photochemistry of the Water Molecule: Adiabatic Versus Nonadiabatic Dynamics. *Acc. Chem. Res.* **2011**, *44*, 369−378.

(6) Jiang, B.; Xie, D.; Guo, H. Communication: State-to-State Differential Cross Sections for $H_2O(B)$ Photodissociation. *J. Chem. Phys.* **2011**, *134*, 231103.

(7) Jiang, B.; Xie, D.; Guo, H. State-to-State Photodissociation Dyanmcis of Triatomic Molecules: H_2O in the *B*-Band. *J. Chem. Phys.* **2012**, *136*, 034302.

(8) Zhou, L.; Jiang, B.; Xie, D.; Guo, H. State-to-State Photodissociation Dynamics of H_2O in the *B*-Band: Competition between Two Coexisting Nonadiabatic Pathways. *J. Phys. Chem. A* **2013**, *117*, 6940−6947.

(9) Douglas, A. E. Electronically Excited States of Ammonia. *Discuss. Faraday Soc.* **1963**, *35*, 158−174.

(10) Vaida, V.; Hess, W.; Roebber, J. L. The Direct Ultraviolet Absorption Spectrum of the $\tilde{A}^1A_2''\leftarrow\tilde{X}^1A_1'$ Transition of Jet-Cooled Ammonia. *J. Phys. Chem.* **1984**, *88*, 3397−3400.

(11) Ziegler, L. D. Rovibrational Absorption Analysis of the $\tilde{A}\leftarrow\tilde{X}$ Transition of Ammonia. *J. Chem. Phys.* **1985**, *82*, 664−669.

(12) Ashfold, M. N. R.; Bennett, C. L.; Dixon, R. N. Dissociation Dynamics of $NH_3(\tilde{A}^1A_2'')$. *Faraday Discuss. Chem. Soc.* **1986**, *82*, 163−175.

(13) Vaida, V.; McCarthy, M. I.; Engelking, P. C.; Rosmus, P.; Werner, H.-J.; Botschwina, P. The Ultraviolet Absorption Spectrum of the $\tilde{A}^1A_2''\leftarrow\tilde{X}^1A_1'$ Transition of Jet-Cooled Ammonia. *J. Chem. Phys.* **1987**, *86*, 6669−6676.

(14) Biesner, J.; Schnieder, L.; Schmeer, J.; Ahlers, G.; Xie, X.; Welge, K. H.; Ashfold, M. N. R.; Dixon, R. N. State Selective Photodissociation Dynamics of $\tilde{A}$ State Ammonia. I. *J. Chem. Phys.* **1988**, *88*, 3607−3616.

(15) Biesner, J.; Schnieder, L.; Ahlers, G.; Xie, X.; Welge, K. H.; Ashfold, M. N. R.; Dixon, R. N. State Selective Photodissociation Dynamics of $\tilde{A}$ State Ammonia. II. *J. Chem. Phys.* **1989**, *91*, 2901−2911.

(16) Ashfold, M. N. R.; Dixon, R. N.; Irvine, S. J.; Koeppe, H.-M.; Meier, W.; Nightingale, J. R.; Schnieder, L.; Welge, K. H. Stereochemical and Angular Momentum Constraints in the Photodissociation of Ammonia. *Philos. Trans. R. Soc. Lond. A.* **1990**, *332*, 375−386.

(17) Woodbridge, E. L.; Ashfold, M. N. R.; Leone, S. R. Photodissociation of Ammonia at 199.3 nm: Rovibrational State Distribution of the $NH_2(\tilde{A}^2A_1)$ Fragment. *J. Chem. Phys.* **1991**, *94*, 4195−4204.

(18) Mordaunt, D. H.; Ashfold, M. N. R.; Dixon, R. N. Photodissociation Dynamics of $\tilde{A}$ State Ammonia Molecules. I. State Dependent μ-v Correlations in the $NH_2(ND_2)$ Products. *J. Chem. Phys.* **1996**, *104*, 6460−6471.

(19) Loomis, R. A.; Reid, J. P.; Leone, S. R. Photofragmentation of Ammonia at 193.3 nm: Bimodal Rotational Distributions and Vibrational Excitation of $NH_2(\tilde{A})$. *J. Chem. Phys.* **2000**, *112*, 658−669.

(20) Reid, J. P.; Loomis, R. A.; Leone, S. R. Characterization of Dynamical Product-State Distributions by Spectral Extended Cross-Correlation: Vibrational Dynamics in the Photofragmentation of NH_2D and ND_2H. *J. Chem. Phys.* **2000**, *112*, 3181−3191.

(21) Bach, A.; Hutchison, J. M.; Holiday, R. J.; Crim, F. F. Photodissociation of Vibrationally Excited Ammonia: Rotational Excitation in the NH_2 Product. *J. Chem. Phys.* **2003**, *118*, 7144−7145.

(22) Bach, A.; Hutchison, J. M.; Holiday, R. J.; Crim, F. F. Competition between Adiabatic and Nonadiabatic Pathways in the Photodissociation of Vibrationally Excited Ammonia. *J. Phys. Chem. A* **2003**, *107*, 10490−10496.

(23) Hause, M. L.; Yoon, Y. H.; Crim, F. F. Vibrationally Mediated Photodissociation of Ammonia: The Influence of N-H Stretching Vibrations on Passage through Conical Intersections. *J. Chem. Phys.* **2006**, *125*, 174309.

(24) Duxbury, G.; Reid, J. P. Renner-Teller Interaction, High Angular Momentum States and Spin-Orbit Interaction in the Electronic Spectrum of ND_2. *Mol. Phys.* **2007**, *105*, 1603−1618.
(25) Wells, K. L.; Perriam, G.; Stavros, V. G. Time-Resolved Velocity Map Ion Imaging Study of NH_3 Photodissociation. *J. Chem. Phys.* **2009**, *130*, 074308.
(26) Rodriguez, J. D.; Gonzalez, M. G.; Rubio-Lago, L.; Banares, L. A Velocity Map Imaging Study of the Photodissociation of the $\tilde{A}$ State of Ammonia. *Phys. Chem. Chem. Phys.* **2014**, *16*, 406−413.
(27) Dixon, R. N. The Stretching Vibrations of Ammonia in Its $\tilde{A}^1A_2''$ Excited State. *Chem. Phys. Lett.* **1988**, *147*, 377−383.
(28) Dixon, R. N. The Influence of Parent Rotation on the Dissociation Dynamics of the $\tilde{A}^1A_2''$ State Ammonia. *Mol. Phys.* **1989**, *68*, 263−278.
(29) Seideman, T. The Predissociation Dynamics of Ammonia: A Theoretical Study. *J. Chem. Phys.* **1995**, *103*, 10556−10565.
(30) Dixon, R. N. Photodissociation Dynamics of $\tilde{A}$ State Ammonia Molecules III. A Three-Dimensional Time-Dependent Calculation Using *Ab Initio* Potential Energy Surfaces. *Mol. Phys.* **1996**, *88*, 949−977.
(31) Dixon, R. N.; Hancock, T. W. R. Recoil Anisotropy following Molecular Predissociation: $NH_3^* \rightarrow H + NH_2$ and $HFCO^* \rightarrow H + FCO$. *J. Phys. Chem. A* **1997**, *101*, 7567−7575.
(32) Bonhommeau, D.; Truhlar, D. G. Mixed Quantum/Classical Investigation of the Photodissociation of $NH_3(\tilde{A})$ and a Practical Method for Maintaining Zero-Point Energy in Classical Trajectories. *J. Chem. Phys.* **2008**, *129*, 014302.
(33) Bonhommeau, D.; Valero, R.; Truhlar, D. G.; Jasper, A. W. Coupled-Surface Investigation of the Photodissociation of $NH_3(\tilde{A})$: Effect of Exciting the Symmetric and Antisymmetric Stretching Modes. *J. Chem. Phys.* **2009**, *130*, 234303.
(34) Lai, W.; Lin, S. Y.; Xie, D.; Guo, H. Non-Adiabatic Dynamics of $\tilde{A}$-State Photodissociation of Ammonia: A Four-Dimensional Wave Packet Study. *J. Phys. Chem. A* **2010**, *114*, 3121−3126.
(35) Yarkony, D. R. Exlporing Molecular Complexity: Conical Intersections and NH_3 Photodissociation. *J. Chem. Phys.* **2004**, *121*, 628−631.
(36) Nangia, S.; Truhlar, D. G. Direct Calculation of Coupled Diabatic Potential-Energy Surfaces for Ammonia and Mapping of a Four-Dimensional Conical Intersection Seam. *J. Chem. Phys.* **2006**, *124*, 124309.
(37) Li, Z. H.; Valero, R.; Truhlar, D. G. Improved Direct Diabatization and Coupled Potential Energy Surfaces for the Photodissociation of Ammonia. *Theo. Chem. Acc.* **2007**, *118*, 9−24.
(38) Zhu, X.; Ma, J.; Yarkony, D. R.; Guo, H. Computational Determination of the $\tilde{A}$ State Absorption Spectrum of NH_3 and of ND_3 Using a New Quasi-Diabatic Representation of the $\tilde{X}$ and $\tilde{A}$ States and Full Six-Dimensional Quantum Dynamics. *J. Chem. Phys.* **2012**, *136*, 234301.
(39) Lai, W.; Lin, S. Y.; Xie, D.; Guo, H. Full-Dimensional Quantum Dynamics of $\tilde{A}$-State Photodissociation of Ammonia. Absorption Spectra. *J. Chem. Phys.* **2008**, *129*, 154311.
(40) Giri, K.; Chapman, E.; Sanz, C. S.; Worth, G. A Full-Dimensional Coupled-Surface Study of the Photodissociation Dynamics of Ammonia Using the Multiconfiguration Time-Dependent Hartree Method. *J. Chem. Phys.* **2011**, *135*, 044311.
(41) Ma, J.; Zhu, X.; Guo, H.; Yarkony, D. R. First Principles Determination of the $NH_2/ND_2(\tilde{A},\tilde{X})$ Branching Ratios for Photodissociation of NH_3/ND_3 via Full-Dimensional Quantum Dynamics Based on a New Quasi-Diabatic Representation of Coupled *Ab Initio* Potential Energy Surface. *J. Chem. Phys.* **2012**, *137*, 22A541.
(42) Xiao, C.; Xu, X.; Liu, S.; Wang, T.; Dong, W.; Yang, T.; Sun, Z.; Dai, D.; Xu, X.; Zhang, D. H.; Yang, X. Experimental and Theoretical Differential Cross Sections for a Four-Atom Reaction: $HD + OH \rightarrow H_2O + D$. *Science* **2011**, *333*, 440−442.
(43) Otto, R.; Ma, J.; Ray, A. W.; Daluz, J. S.; Li, J.; Guo, H.; Continetti, R. E. Imaging Dynamics on the $F + H_2O \rightarrow HF + OH$ Potential Energy Surfaces from Wells to Barriers. *Science* **2014**, *343*, 396−399.
(44) Zhu, X.; Yarkony, D. R. Fitting Coupled Potential Energy Surfaces for Large Systems: Method and Construction of a 3-State Representation for Phenol Photodissociation in the Full 33 Internal Degrees of Freedom Using Multireference Configuration Interaction Determined Data. *J. Chem. Phys.* **2014**, *140*, 024112.
(45) Guo, H. A Time-Independent Theory of Photodissociation Based on Polynomial Propagation. *J. Chem. Phys.* **1998**, *108*, 2466−2472.
(46) Ma, J.; Guo, H. Full-Dimensional Quantum State Resolved Predissociation Dynamics of HCO_2 Prepared by Photodetaching HCO_2^-. *Chem. Phys. Lett.* **2011**, *511*, 193−195.
(47) Guo, H. Recursive Solutions to Large Eigenproblems in Molecular Spectroscopy and Reaction Dynamics. *Rev. Comput. Chem.* **2007**, *25*, 285−347.
(48) Dixon, R. N.; Irving, S. J.; Nightingale, J. R. Transitions between States of High Angular-Momentum in the Electronic-Spectrum of NH_2. *J. Chem. Soc. Faraday Trans.* **1991**, *87*, 2121−2133.
(49) Zhu, X.; Yarkony, D. R. On the Representation of Coupled Adiabatic Rotential Energy Surfaces Using Quasi-Diabatic Hamiltonians: Description of Accidental Seams of Conical Intersection. *Mol. Phys.* **2010**, *108*, 2611−2619.